



Systemic immune response to vimentin and granuloma formation in a model of pulmonary sarcoidosis

Harini Bagavant^a, Katarzyna Cizio^a, Antonina M. Araszkiwicz^a, Joanna A. Papinska^b,
Lori Garman^c, Chuang Li^c, Nathan Pezant^c, Wonder P. Drake^d, Courtney G. Montgomery^c,
Umesh S. Deshmukh^{a,*}

^a Arthritis and Clinical Immunology Program, Oklahoma Medical Research Foundation, Oklahoma City, OK, USA

^b Department of Microbiology and Immunology, University of Oklahoma, Health Sciences Center, Oklahoma City, OK, USA

^c Genes and Human Disease Research Program, Oklahoma Medical Research Foundation, Oklahoma City, OK, USA

^d Division of Infectious Diseases, Department of Medicine, Department of Pathology, Microbiology, and Immunology, Vanderbilt University School of Medicine, Nashville, TN, USA

ARTICLE INFO

Keywords:

Sarcoidosis
Mouse models
Vimentin
Granuloma
Type 2 innate lymphoid cells
Multinucleated giant cells

ABSTRACT

A characteristic feature of sarcoidosis is a dysregulated immune response to persistent stimuli, often leading to the formation of non-necrotizing granulomas in various organs. Although genetic susceptibility is an essential factor in disease development, the etiology of sarcoidosis is not fully understood. Specifically, whether autoimmunity contributes to the initiation or progression of the disease is uncertain. In this study, we investigated systemic autoimmunity to vimentin in sarcoidosis. IgG antibodies to human vimentin were measured in sera from sarcoidosis patients and healthy controls. Mice immunized with recombinant murine vimentin were challenged intravenously with vimentin-coated beads to mimic pulmonary sarcoidosis. Lungs from treated mice were studied for cellular infiltration, granuloma formation, and gene expression. Immune cells in the bronchoalveolar lavage fluid were evaluated by flow cytometry. Compared to healthy controls, sarcoidosis patients had a higher frequency and levels of circulating anti-vimentin IgG. Vimentin-immunized mice developed lung granulomas following intravenous challenge with vimentin-coated beads. These sarcoidosis-like granulomas showed the presence of Langhans and foreign body multinucleated giant cells, CD4 T cells, and a heterogeneous collection of MHC II positive and arginase 1-expressing macrophages. The lungs showed upregulated pro-inflammatory gene expression, including *Irfng*, *Il17*, and *Tnfa*, reflecting TH1/TH17 responses typical of sarcoidosis. In addition, genes in the TH2 canonical pathway were also upregulated, congruent with increased numbers of ILC2 in the bronchoalveolar lavage. Overall, these results further validate vimentin as an autoantigen in sarcoidosis and provide evidence for an anti-vimentin immune response in disease pathogenesis. Our study also highlights the possible role of ILC2-driven TH2-like responses in the formation of lung granulomas in sarcoidosis.

1. Introduction

Sarcoidosis is a chronic, debilitating, multi-organ disease commonly affecting the lungs, skin, lymphatics, heart, and brain [1]. The hallmark of sarcoidosis is the presence of non-necrotizing granulomas consisting of T cells, macrophages, epithelioid cells, and multinucleated giant cells. Although genetic susceptibility is an essential factor in the development of sarcoidosis, the etiology of the disease remains unresolved [2]. Infections or autoimmunity are viewed as potential triggers. Sarcoidosis granulomas may be formed as a result of an immune response that is

unable to clear microbes or microbial products from target organs [3]. Indeed, a recent report identified T cell epitopes on airborne organisms as targets for CD4 T cells in bronchoalveolar (BAL) fluid of sarcoidosis patients, suggesting microbial exposure as an essential environmental factor in sarcoidosis [4]. However, while some patient studies have demonstrated an unambiguous presence of *Mycobacterium*, *Propionibacterium*, or their products in the granuloma, other reports showed a complete lack of any unique microbial signature [5,6]. These conflicting results suggest the possibility of other etiologic mechanisms like autoimmunity, supported by the increased frequencies of auto-reactive CD4

* Corresponding author. Arthritis and Clinical Immunology, Oklahoma Medical Research Foundation, USA.

E-mail address: umesh-deshmukh@omrf.org (U.S. Deshmukh).

<https://doi.org/10.1016/j.jtauto.2022.100153>

Received 1 December 2021; Received in revised form 10 March 2022; Accepted 30 March 2022

Available online 5 April 2022

2589-9090/© 2022 The Authors. Published by Elsevier B.V. This is an open access article under the CC BY-NC-ND license (<http://creativecommons.org/licenses/by-nc-nd/4.0/>).

Table 1
Demographics of Sarcoidosis patients and healthy controls.

	Healthy Controls	Sarcoidosis Patients	p-value
Total, n	13	48	
Females, n (%)	8 (61.5%)	27 (56.3%)	ns
Age in years median (range)	26 (22–32)	55 (29–72)	p < 0.0001
Race, n (%)			ns
African American	2 (15.4%)	15 (31.3%)	
European American	11 (84.6%)	32 (66.7%)	
Not disclosed		1 (2.1%)	

T cells in patients [7], and a positive Kveim reagent skin test that was previously used to diagnose sarcoidosis [8]. The Kveim reagent skin test is a delayed-type hypersensitivity response to an extract from sarcoidosis patient spleen. Proteomic analysis of the Kveim reagent showed the presence of numerous proteins, of which vimentin, an intermediate filamentous cytoskeletal protein, was identified as a potential candidate autoantigen [9].

Elevated antibodies to citrullinated vimentin are diagnostic of several autoimmune diseases, including SLE, rheumatoid arthritis, Crohn's disease, idiopathic pulmonary fibrosis, and ankylosing spondylarthritis [10]. Vimentin undergoes multiple post-translational modifications, and that could potentially contribute to its immunogenicity. Indeed, a recent study showed that antibodies to modified citrullinated vimentin were increased in sarcoidosis and tuberculosis [11]. Previously, it was reported that patients with Lofgren's syndrome, an acute, self-limiting presentation of sarcoidosis, harbor both vimentin-reactive CD4 T cells as well as anti-vimentin IgG and IgA antibodies in their BAL fluid [12]. Despite these observations, the role of vimentin as a *bona fide* pathogenic autoantigen in sarcoidosis is open to debate [13]. To address this issue, we investigated whether a systemic immune response to vimentin is pathogenic in sarcoidosis. Anti-vimentin IgG levels were measured in sera from sarcoidosis patients and healthy controls, and the ability of an anti-vimentin immune response to induce sarcoidosis-like granulomas was tested using a mouse model.

2. Materials and methods

2.1. Patients and controls

This study was performed following the Helsinki Declaration and approved by the Oklahoma Medical Research Foundation (OMRF) and Vanderbilt University Medical Center (VUMC) Institutional Review Boards. Informed consent was obtained for experimentation with human subjects. Banked serum samples were obtained from sarcoidosis patients and healthy volunteers seen at VUMC. Adults aged >18 years with sarcoidosis diagnosis as defined by the 2020 American Thoracic Society/European Respiratory Society/World Association of Sarcoidosis and Other Granulomatous Disorders statement on sarcoidosis were eligible for enrollment [14]. Participants were also selected based on demonstration of pulmonary disease progression according to at least one of the following three criteria: (1) decline of the absolute percentage of predicted forced vital capacity or diffusing capacity for carbon monoxide of at least 5% on serial measurements over 24 months; (2) radiographic progression in chest imaging on side-by-side comparison; or (3) decline in dyspnea score, as measured by using the Transition Dyspnea Index. The demographics of sarcoidosis patients (n = 48) and healthy controls (n = 13) are shown in Table 1.

2.2. Detection of anti-vimentin antibodies

Anti-vimentin antibodies were measured by a standard ELISA against

recombinant human vimentin purified from a baculovirus expression system (SinoBiological, Wayne, PA, USA). Vimentin in bicarbonate buffer (5 µg/mL, pH 9.4, was coated on ELISA plates overnight at 4 °C. All sera were tested at a 1:100 dilution. Serial dilutions of a pooled serum sample were used as a calibrator for each plate. Bound antibody was detected with HRP-conjugated goat anti-human IgG (SouthernBiotech, Birmingham AL, USA), and the enzyme activity was determined with an o-phenylenediamine dihydrochloride (OPD) peroxidase substrate (Sigma-Aldrich, St. Louis, MO, USA). The reaction was stopped with 2.5 N sulfuric acid. Results are presented as absorbance at 490 nm. The mean O.D. +2SD of the control group was used as a cut-off to determine the prevalence of anti-vimentin antibodies.

2.3. Mice, granuloma induction, and tissue collection

All experiments were approved by the OMRF Institutional Animal Care and Use Committee and followed the National Institutes of Health guidelines. Lung granulomas were induced as previously reported [15, 16] with some modifications. Female C57BL/6 mice were obtained from Jackson Laboratories (Bar Harbor, ME, USA) and housed under specific pathogen-free conditions. Mice (10–13 wk old) were immunized subcutaneously with recombinant 6X Histidine tag-murine vimentin (6XHis-mVim) (50 µg/mouse; n = 7) in Complete Freund's adjuvant (Pierce Chemical, Dallas, TX, USA). Control mice received saline-CFA emulsion (n = 6). On day 10 post-immunization, all mice were challenged intravenously with 6XHis-mVim bound to Ni-NTA agarose beads (40 µm diameter, ~20,000 beads/mouse). The mice were euthanized on day 15. BAL fluid was collected for immune cell analysis by flow cytometry. Lungs were preserved in 10% neutral buffered formalin for histopathology, 1% Paraformaldehyde-lysine-periodate (PLP) for cryo-sectioning, and snap-frozen in liquid nitrogen for gene expression analysis. The experiments were carried out in two cohorts of mice, and the results are pooled from two independent experiments.

2.3.1. Purification of mouse recombinant protein

The plasmid pReceiver-B01 expressing mouse *Vim* (NM_011701.4) with an N-terminal-6XHis tag was purchased from GeneCopoeia, Inc (Rockville, MD). Recombinant 6XHis-mVim was produced in *E. coli* and purified on Ni-NTA agarose column (Qiagen, Germantown, MD) under denaturing conditions by following the manufacturer's instructions. To prepare vimentin-coupled beads, 2 mg of purified protein was dissolved in an 8 M Urea buffer containing 10 mM β-Mercaptoethanol and mixed with 100 µl of Ni-NTA agarose beads (Cube Biotech, Monheim, Germany). After 2 h of end-to-end mixing, the beads were washed with successively decreasing Urea (8 M–1 M), followed by three washes with PBS. Finally, the beads were suspended in PBS, sterilized by irradiation, and stored at 4 °C.

2.4. Lung histopathology analyses

Formalin-fixed paraffin-embedded lung sections were stained with Hematoxylin and Eosin. Images were scanned on an Aperio CS2 digital scanner, and image analysis was performed using Aperio Imagescope software (Leica Biosystems, Buffalo Grove, IL, USA). The length (in microns) at the widest portion of the granuloma and going through a bead was measured to determine granuloma size. Multinucleated giant cells were counted using QuPath 3.0 software [17]. Cells ≥3 nuclei/cell classified as Langhans (rounded cells with nuclei arranged along cell margin) or Foreign body (large cells of variable shapes with randomly arranged nuclei) were used for training, and the annotations were applied to the entire image. Cells were counted in four distinct regions of 1.25 mm² each. The numbers were verified independently by 2 investigators (KC, HB).

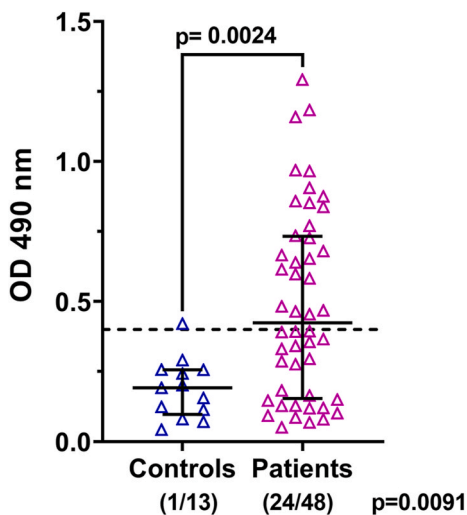


Fig. 1. Anti-vimentin IgG levels in sera from healthy controls and sarcoidosis patients. The reactivity to human vimentin was determined by ELISA. All sera were tested at 1:100 dilution. Data are plotted as absorbance at 490 nm. Each data point represents one serum sample. The mean O.D. +2SD of the control group was used as a cut-off for positivity and is indicated by the dotted line. The number of patients positive/total for each group is shown in parentheses.

2.5. Immune cells in BAL fluid by flow cytometry

BAL was performed by infusing 1 ml of DMEM through a tracheal cannula. The cells in the BAL fluid were recovered by centrifugation, and RBCs were lysed with Tris-buffered ammonium chloride. Cells were counted and were stained for different markers to identify immune cell populations using standard flow cytometry protocols. Antibodies used are listed in [Supplementary Table 1](#). The data were acquired on a BD FACS Celesta using BD FACSDiva software (Becton Dickinson and Co, Franklin Lakes, NJ, USA) and analyzed using FlowJo software.

2.6. Immunostaining for immune cell infiltrates

Lungs fixed in 1% PLP were floated through 30% sucrose, processed for cryo-sectioning, and stained for immune cell markers using

antibodies listed in [Supplementary Table 1](#). Briefly, sections were treated with 0.3% Triton X100 in PBS and incubated overnight at 4 °C with cocktails of fluorochrome-conjugated antibodies in 1% BSA in PBS. For detection of CD68, iNOS, and arginase 1, the sections were incubated with primary antibodies overnight at 4 °C, followed by fluorochrome-conjugated secondary antibodies. The nuclei were stained with DAPI and sections mounted in Prolong Gold. Images were captured on a confocal microscope (Carl Zeiss Microscopy LLC, White Plains, NY, USA).

2.7. Gene expression analysis

RNA was isolated using RNeasy mini kit (Qiagen, Germantown MD, USA), and gene expression was determined using nCounter Mouse Immunology Panel with 549 genes, 14 housekeeping genes, and 14 positive and negative system controls (NanoString Technologies, Seattle, WA, USA). Normalized gene expression values were obtained using nSolver software (NanoString Technologies).

2.8. Statistical analyses

Prism 9.0 software (GraphPad, San Diego, CA, USA) was used for all analyses. Normality tests were performed on each dataset to determine Gaussian distributions. The student's t-test was used to compare means between adjuvant control and vimentin-immunized groups. For non-Gaussian distributions, the Mann-Whitney test was used to determine differences between groups, and Spearman's test was used to determine correlation coefficients. The significance of disease incidence was assessed using Fisher's exact test. A value of $p < 0.05$ was considered to be statistically significant.

3. Results

3.1. Increased levels of anti-vimentin IgG in sarcoidosis patient sera

IgG antibodies to human vimentin were measured in sera of sarcoidosis patients ($n = 48$) and healthy controls ($n = 13$). Compared to healthy controls, sarcoidosis patients showed a wider range of reactivity to vimentin and significantly ($p = 0.0024$) higher anti-vimentin IgG levels ([Fig. 1](#)). Further, the prevalence of anti-vimentin IgG positivity in patients was greater than controls (24/48: 50% versus 1/13: 7.6% respectively; $p = 0.0091$). These data demonstrate the presence of a

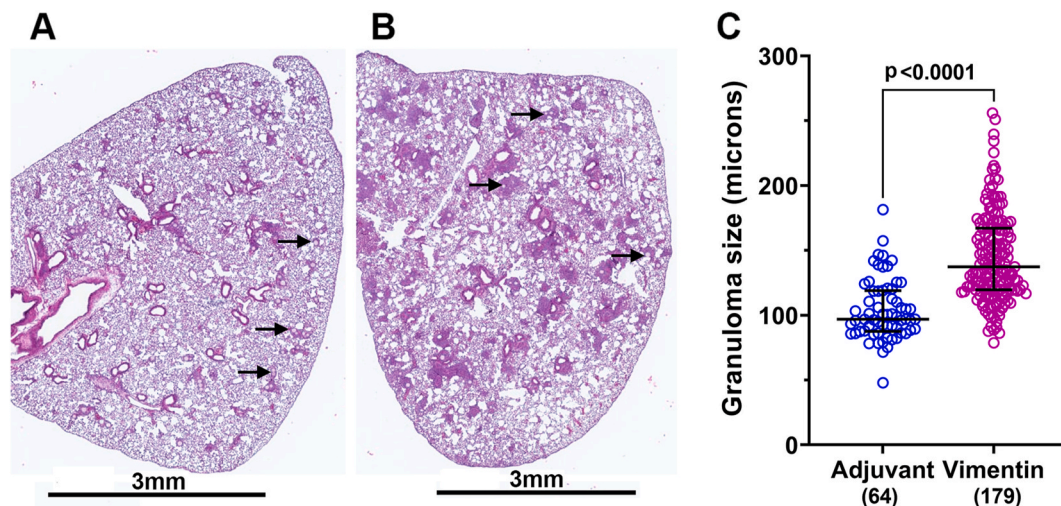


Fig. 2. Lung granulomas in vimentin-immunized mice. Representative images of lung sections from adjuvant control (A) and vimentin-immunized (B) mice are shown. All mice showed the presence of 6XHis-mVim-coated beads in the lung sections (arrows). (B) Note numerous large and small areas of inflammation throughout the lung in vimentin-immunized mice. Scale bar = 3 mm. (C) The diameter of granulomas measured in one cross-section of the lung is shown. The number of granulomas counted in each group is indicated in parenthesis.

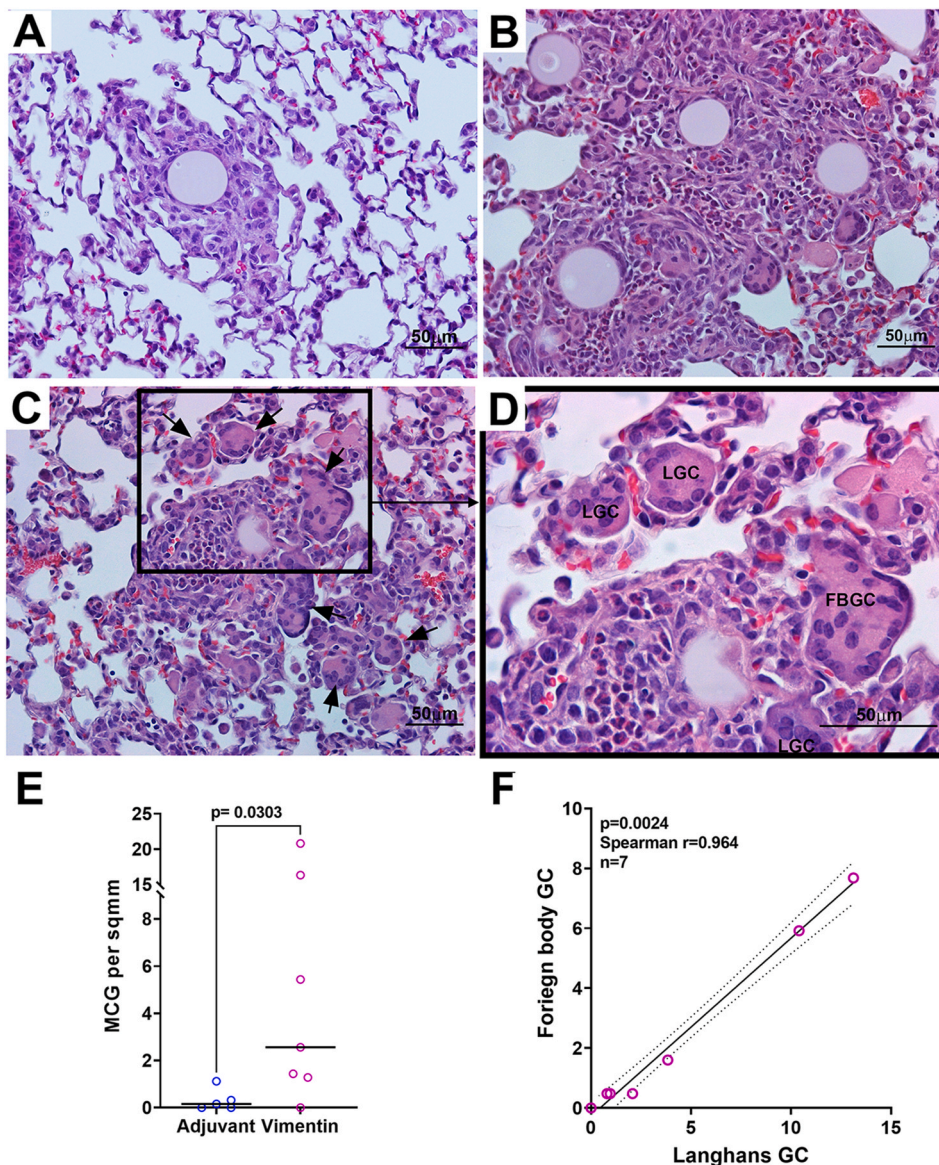


Fig. 3. Multinucleated giant cells are readily detected in lung granulomas. Representative images of H&E stained lung sections from adjuvant control (A) and vimentin-immunized (B–D) mice are shown. (C) Multinucleated giant cells (MGC) are seen in and around the granuloma (arrows) and are increased in vimentin-immunized mice. (D) A higher magnification image of inset in C showing Langhans (LGC) and Foreign body giant cells (FBGC) in the granulomas. Scale bar = 50 μ m. (E) The number of MGC was quantified in 4 discrete areas of 1.25 mm^2 in one section for each mouse, and the results are represented as MGC per sq mm. (F) A robust correlation between the numbers of Foreign body and Langhans GC is noted in vimentin-immunized mice.

systemic autoimmune response targeting vimentin in sarcoidosis patients. Although the healthy controls in our cohort were significantly younger ($p < 0.001$) (Table 1), there was no correlation between age and anti-vimentin antibody levels in patients ($r = -0.126$, $p = 0.3934$). Furthermore, reactivity to vimentin did not differ by self-reported race ($p = 0.636$) or gender ($p = 0.899$).

3.2. Lung granulomas form in vimentin-immunized mice

To determine whether an autoimmune response to vimentin can induce granuloma formation, C57BL/6 female mice ($n = 7$) were immunized with recombinant 6XHis-mVim protein in CFA. Mice ($n = 6$) injected with saline in CFA served as controls. On day 10, all mice were challenged intravenously with 6XHis-mVim bound to Ni-NTA agarose beads. Immunization and granuloma formation were reproduced in two different cohorts of mice and the results presented are pooled from two independent experiments. As previously reported, the beads were trapped in the pulmonary vascular bed and were detected in lung sections (Fig. 2) [16]. In the adjuvant controls, the beads induced foreign body granulomas with inflammation limited to areas around the beads (Figs. 2A and 3A). The granulomas in the vimentin-immunized mice

were significantly larger (Figs. 2B and 3B) and spread out over the entire lobe, with normal lung tissue seen interspersed between the inflammatory foci (Fig. 2B). The diameter of each granuloma in a section was measured as the distance passing through the center of the bead and covering the widest part of the inflammation around the bead. Granulomas in vimentin-immunized mice ($144.7 \pm 2.53 \mu\text{m}$, $n = 179$) were significantly larger than those in the adjuvant controls ($104.0 \pm 2.93 \mu\text{m}$, $n = 64$; $p < 0.0001$) (Fig. 2C).

Consistent with the known characteristics of sarcoidosis, vimentin-immunized mice showed the presence of multinucleated giant cells (MGC) distributed throughout the granulomas at numbers (7.97 ± 3.45 per sq mm) that were significantly higher than adjuvant controls (0.533 ± 0.297 per sq mm; $p < 0.05$) (Fig. 3C–E). Both Langhans and foreign body MGC were seen. Further, the numbers of the two different MGC types were significantly correlated (Fig. 3F, Spearman $r = 0.941$, $p = 0.0167$), mirroring the reports describing mediastinal lymph node granulomas from sarcoidosis patients [18].

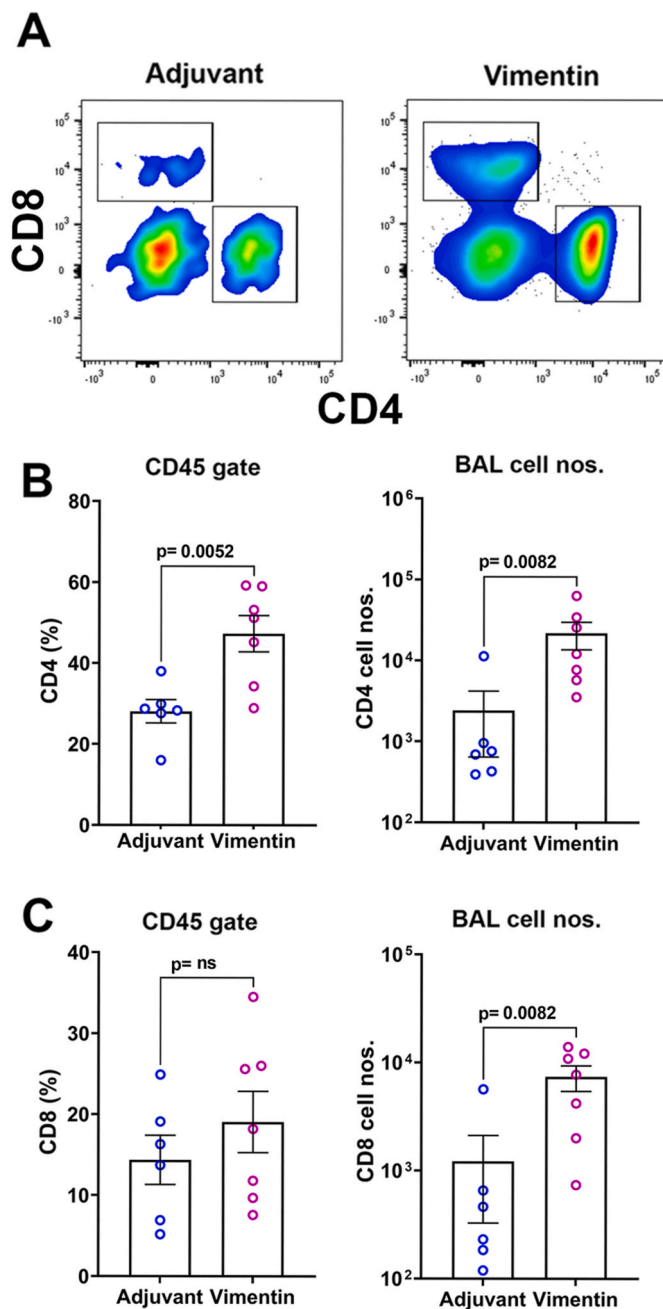


Fig. 4. Analysis of CD4 and CD8 T cells in BAL fluid. (A) Analysis of immune cells in BAL fluid showing representative flow cytometry plots for CD4 and CD8 cells within a live CD45⁺ gate. Frequencies and total numbers of CD4 T cells (B) and CD8 T cells (C) in BAL fluid from adjuvant control and vimentin-immunized mice.

3.3. Organization of immune cells in a vimentin-induced sarcoidosis-like granuloma

Lung granulomas consisting of CD4 T cells and activated macrophages, accompanied by increased T cells in the BAL fluid, are critical attributes of sarcoidosis [19]. Flow cytometry analysis of BAL fluid in vimentin-immunized mice showed higher numbers of CD45⁺ immune cells ($4.3 \pm 1.5 \times 10^4$, $n = 7$) compared to adjuvant controls ($0.7 \pm 0.5 \times 10^4$, $n = 6$; $p = 0.0082$). CD4 T cells constituted a major fraction of these CD45⁺ cells, and the CD4 T cell frequencies were higher in the vimentin-immunized compared to adjuvant controls (Fig. 4A and B). Although the CD8 T cells frequencies did not differ between the groups,

significantly higher CD8 T cell numbers were recovered in the BAL fluid of vimentin-immunized mice over adjuvant controls (Fig. 4C).

Immunofluorescence staining of lung sections was performed to characterize the immune cells in granulomas. Adjuvant-treated mice did not show significant infiltration of T cells, F4/80 macrophages, or upregulated MHC II expression (Fig. 5 A–C). In contrast, lungs from vimentin-immunized mice showed that CD4 cells were the predominant T cells in the granuloma, although a few CD8 T cells were also present (Fig. 5D). An increase in antigen-presenting cells expressing MHC II was noted in the areas infiltrated with the CD4 T cells (Fig. 5E). A significant proportion of the MHC II positive cells were F4/80 macrophages (Fig. 5F).

Arginase 1-expressing M2 macrophages, enriched in pulmonary sarcoidosis, play an essential role in epithelioid transformation, a vital step for the organization of the granuloma architecture [20,21]. To determine macrophage polarization, adjacent sections from each lung were stained for the presence of iNOS or Arginase 1 and the macrophage marker CD68 (Fig. 6). Some iNOS positive cells were seen in the adjuvant control granulomas (Fig. 6A). Vimentin-immunized mice showed larger numbers of iNOS positive cells in the granuloma and the surrounding tissue (Fig. 6C). Only vimentin-immunized mice showed CD68⁺ arginase 1-expressing cells prominently along the outer edges of the granuloma as well as interspersed within the granuloma (Fig. 6D). CD68⁺ cells in adjuvant-treated mice did not show the presence of arginase 1 (Fig. 6B).

3.4. Enrichment of inflammatory, TH1, and TH2 canonical pathways in granulomatous lungs

Lung RNA was isolated from adjuvant control ($n = 3$) and vimentin-immunized ($n = 5$) mice, and gene expression was studied using the nCounter Immunology panel (Nanostring Technologies, Seattle WA, USA). The nSolver analysis showed that of the 549 immune-related genes studied, the expression of 203 genes was significantly (p -value < 0.05) different between the two groups (Supplementary Table 2). Vimentin-immunized mice showed 168 upregulated (Fold Change > 1.5) and 11 downregulated genes (Fold Change < 1.5) (Fig. 7A). As presented in Table 2, the genes exhibiting a > 1.5 fold change included chemokines (*Ccl2*, *Ccl3*, *Ccl7*, *Ccl8*, *Ccl9*, *Ccl12*, *Ccl24*, *Cxcl1*, and *Cxcl3*) and chemokine receptors (*Ccr2*, *Ccr3*, *Ccr4*, *Ccr5*, and *Ccr8*), supporting the increase in immune cell trafficking to the lungs. In addition, significant upregulation of MHC II genes, including *H-2Eb1* ($2.69x$, $p = 1.6 \times 10^{-4}$) and *H-2Ab1* ($2.14x$, $p = 8.8 \times 10^{-4}$), reinforce the role of CD4 T cells and antigen-presenting cells in granuloma formation. Of note was also the increase in immune-regulatory genes *Pdcdlg2*, *Pdcd1*, *Foxp3*, and *Ctla4*. In sarcoidosis patients, upregulation of PD1 (encoded by *Pdcd1*) on CD4 T cells and accumulation of Foxp3^{bright} T regulatory cells in granulomas correlates with increased interstitial fibrosis [22,23].

Ingenuity pathway analysis (Qiagen) of the gene expression data showed the highest enrichment of genes within the canonical neuro-inflammation signaling pathway, followed by the TH1 and TH2 pathways (Fig. 7B). Immunization in CFA drives a TH1/TH17 skewed CD4 T cell response. Indeed, we noticed a significantly increased expression of *Ifng* and *Il17* in the lungs of vimentin-immunized mice (Fig. 7C). Furthermore, there was a 2.21x increase ($p = 1.5 \times 10^{-5}$) in *Tnfrsf8* (CD30L), which was accompanied by a corresponding increase in the expression of *Tnfrsf8* (CD30) ($1.4x$, $p = 0.04$) (Fig. 7A, Supplementary Table 2). This observation is significant, as CD30L is upregulated on TH1 polarized antigen-specific T cells in *M. tuberculosis* infection, and a blockade of CD30 prevents allergic TH2 mediated inflammation in the lungs [24,25].

Of the 137 genes in the IPA-defined canonical TH2 pathway, expression of 41 genes was significantly different between adjuvant control and vimentin-immunized groups (ratio = 0.299, z score = 4.017; p value = 10^{-49}). Some of the canonical TH2 pathway genes like *Il4*, *Il5*, *Il10*, *Il13*, and *Il33* were significantly upregulated in the lungs of

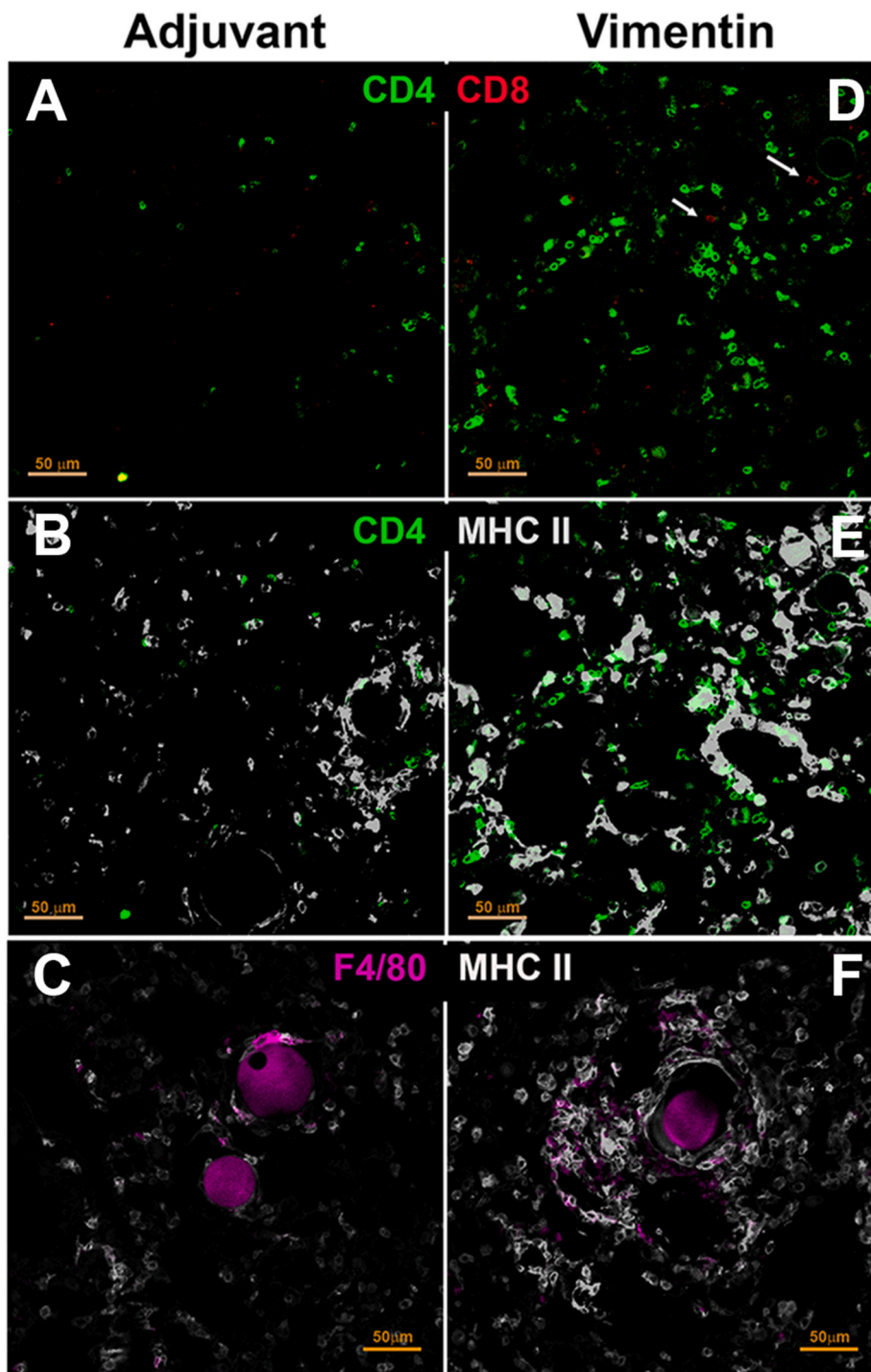


Fig. 5. Immunohistochemical analysis of immune cells in lung granulomas. Immunostaining of lung sections from adjuvant control (A–C) and vimentin-immunized mice (D–F). Vimentin immunized mice showed (D) prominent CD4 T cell infiltrates with few CD8 T cells (arrows). (E) The CD4 T cells were closely associated with MHC II positive cells. (F) F4/80+ macrophages were seen surrounding the beads and showed upregulation of MHC II. Adjuvant control lungs (A–C) showed fewer CD4 T, CD8 T cells, MHC II positive cells, and F4/80 macrophages.

vimentin-immunized mice (Fig. 7C). In addition, the expression of *Intelectin 1* (*Itn1*), a type 2 associated molecule upregulated in epithelial cells by IL-33, was also higher (18.02x, $p = 0.0362$) (Fig. 7A), further supporting the presence of a TH2 environment [26]. We thus investigated the presence of type 2 innate lymphoid cells (ILC2) in BAL fluid as a potential contributor to the TH2 response. Flow cytometry analysis showed a significant increase in the frequency and numbers of ILC2 in the BAL of the vimentin-immunized mice over adjuvant controls (Fig. 8).

4. Discussion

Sarcoidosis is considered a dysregulated immune response to a

persistent stimulus that results in granuloma formation in genetically susceptible individuals [1,13]. Our study supports the role of autoimmunity in the etiology of sarcoidosis. In this study, we demonstrate that circulating autoantibodies reactive with vimentin are present in sarcoidosis patients. Using a mouse model, we also show that an immune response to vimentin can induce sarcoidosis-like granulomas and cytokine responses in the lung. Furthermore, our study suggests that innate immunity, specifically ILC2, in the target organ may play an essential role in disease pathogenesis.

Vimentin is a well-established target autoantigen in several autoimmune diseases like SLE and RA [10]. In sarcoidosis, anti-vimentin reactivity is reported in patients with Lofgren's syndrome (an acute

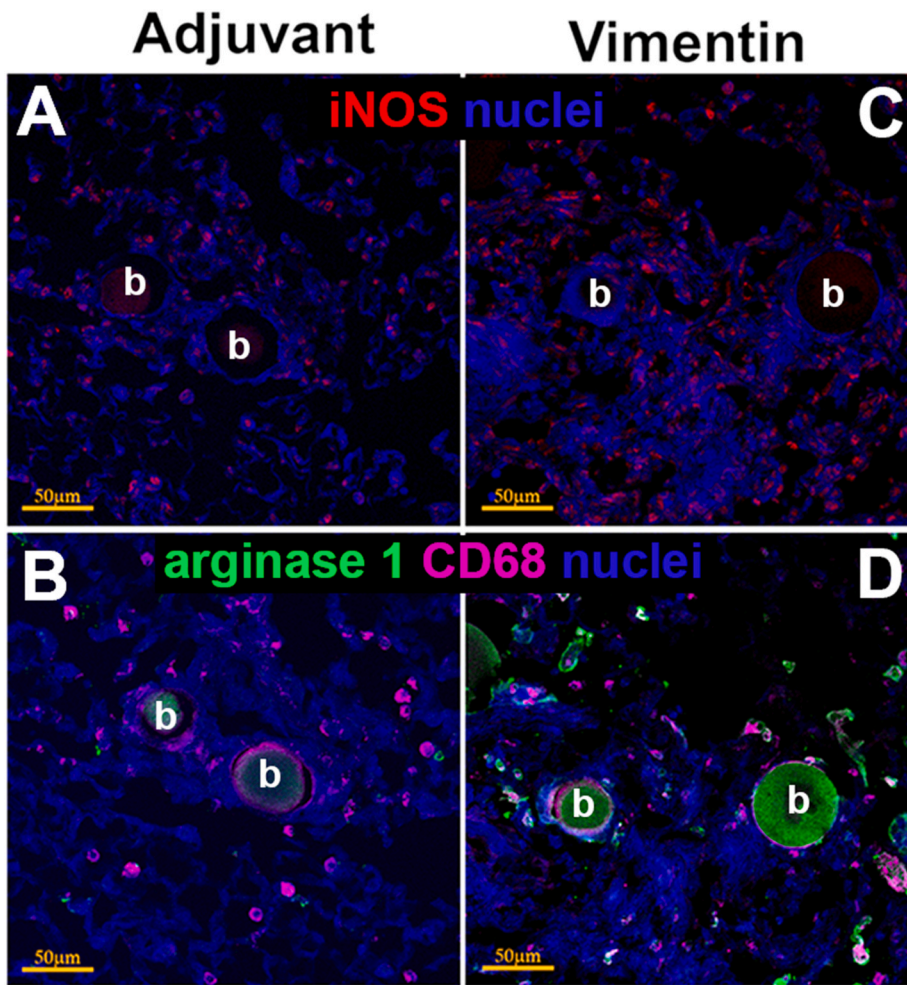


Fig. 6. Characterization of macrophages in lung granulomas. Immunostaining of adjacent sections of lungs from adjuvant control (A,B) and vimentin-immunized mice (C,D). iNOS producing cells were present in granulomas from both groups (A,C). However, only vimentin-immunized mice show CD68⁺ macrophages expressing arginase 1, suggesting M2 polarization, interspersed throughout and along the outer margins of the granuloma (D). CD68 positive cells were present around beads in the adjuvant control and did not express arginase 1 (C). Scale bar = 50 μm; b, beads.

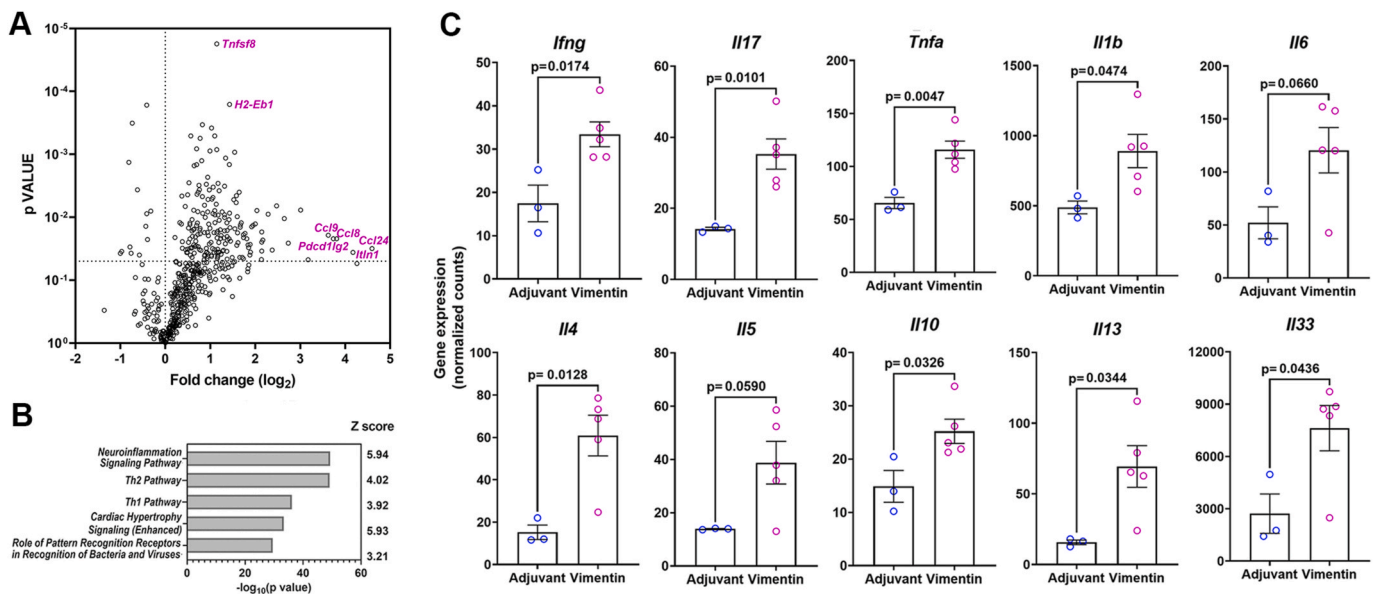


Fig. 7. Inflammatory gene expression in lungs from adjuvant control and vimentin-immunized mice. (A) Volcano plot showing fold change in gene expression in lungs of adjuvant control and vimentin-immunized mice. The 5 maximally and 2 most significantly upregulated genes are identified. (B) The top 5 canonical pathways significantly enriched by Ingenuity Pathway Analysis (Qiagen). (C) Expression levels of representative TH1 and TH2 cytokine genes in lungs.

Table 2
Differentially expressed genes in lungs from adjuvant controls and vimentin-immunized mice.

Category	GENE	Linear fold change	p-value	
CC chemokines	<i>Ccl2</i>	3.61	0.030	
	<i>Ccl3</i>	3.17	0.014	
	<i>Ccl4</i>	2.02	0.025	
	<i>Ccl7</i>	4.87	0.009	
	<i>Ccl8</i>	14.02	0.022	
	<i>Ccl9</i>	12.33	0.019	
	<i>Ccl12</i>	2.67	0.011	
	<i>Ccl24</i>	24.18	0.031	
	CXC chemokines	<i>Cxcl1</i>	3.86	0.013
		<i>Cxcl3</i>	3.69	0.027
Chemokine receptors		<i>Ccr2</i>	2.98	0.006
	<i>Ccr3</i>	9.03	0.048	
	<i>Ccr4</i>	4.4	0.047	
	<i>Ccr5</i>	8.05	0.008	
	<i>Ccr8</i>	3.22	0.012	
Immuno-regulatory genes	<i>Pdcd1lg2</i>	4.1	0.008	
	<i>Pdcd1</i>	13.32	0.022	
	<i>Ctla4</i>	2.49	0.003	
	<i>Foxp3</i>	2.28	0.025	

Selected genes with >1.5x upregulation and $p < 0.05$.

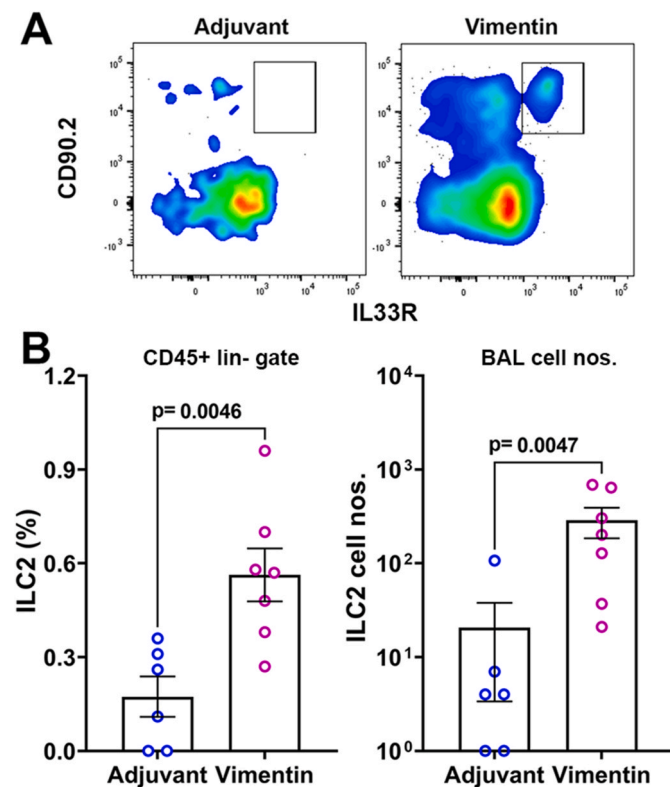


Fig. 8. Type 2 innate lymphoid cells in BAL fluid. (A) Representative flow cytometry plots for ILC2 (CD90 and IL-33R positive) in CD45⁺ lineage negative gate in adjuvant control and vimentin-immunized mice. (B) Frequencies and the total number of ILC2 cells were significantly higher in BAL fluid from vimentin-immunized mice.

form of sarcoidosis almost exclusively seen in persons of European descent) who also carry HLADRB1*0301, a haplotype strongly associated with protection from chronic disease in Caucasians. These studies suggest that patients with the greatest likelihood of a self-limiting disease develop a local immune response to vimentin [27]. However, our analysis of anti-vimentin antibodies in patients visiting the VUMC suggests that patients with acute and chronic clinical courses exhibit an immune response to vimentin. Furthermore, the incidence of

anti-vimentin IgG was not different between self-reported African American (7/15; 46.7%) and European American (16/32; 50%) sarcoidosis patients. A recent report showing elevated levels of antibodies to modified citrullinated vimentin in sarcoidosis patients from a Russian cohort also makes a strong case for an autoimmune etiology for sarcoidosis [11]. In our study, reactivity of human sera was tested against recombinant vimentin protein generated in a eukaryotic expression system, and was not experimentally citrullinated. Collectively, these results suggest that anti-vimentin antibodies recognize the native and modified citrullinated protein and are readily detected in a broad subset of sarcoidosis patients. However, considering that antibody responses to modified citrullinated vimentin are detected in several autoimmune disorders [10], the presence of anti-vimentin antibodies in sarcoidosis patients is not a diagnostic tool for sarcoidosis. Instead, it provides evidence for the involvement of autoimmunity in sarcoidosis. Clearly, screening additional sarcoidosis patient cohorts from different geographical locations for anti-vimentin antibodies will further validate vimentin as a legitimate autoantigen in sarcoidosis.

The unknown environmental triggers, complex genetic factors, and diverse cellular composition of the granuloma contribute to the challenges of mimicking the entire clinical spectrum of sarcoidosis in animals [28]. Nevertheless, different aspects of the disease have been successfully modeled using infectious agents like *P. acnes*, bacterial peptides from mycobacterial superoxide dismutase (SOD), inorganic particles like multi-walled carbon nanotubes, and genetic manipulations like PPAR γ or tuberous sclerosis protein 2 deficiency [16,29–33]. Our study demonstrates that mice sensitized with murine vimentin develop sarcoidosis-like granulomas in the lung following a challenge with vimentin-coated beads. This experimental mouse model system has some similarities with a previous report of a bacterial antigen-specific granuloma where mice immunized with a mycobacterial SOD synthetic peptide were challenged with the peptide covalently coupled to Sepharose 4B beads (40–200 μ m diameter) [16]. However, there are several differences between the two model systems: the induction of an immune response to an autoantigen versus a bacterial peptide, the use of smaller Ni-NTA agarose beads (40–70 μ m diameter), and the non-covalent coupling method for delivery of the antigenic challenge. His-tagged proteins are released from the Ni-NTA beads at acidic pH (<6.0), and any beads or fragments phagocytosed by macrophages would be expected to release the proteins in the acidic lysosomal compartment. Thus, these proteins would be efficiently made available for antigen processing and presentation on the MHC II, thereby recruiting vimentin-reactive T cells around the bead.

In sarcoidosis patients, granulomas in spleens show vimentin-rich areas [9]. Although vimentin is an intracellular, cytoskeletal, filamentous protein, it is secreted from the cells in response to different inflammatory stimuli [34,35]. Thus, extracellular vimentin in sarcoidosis granulomas might be potentially released from macrophages and other inflammatory cells [9]. These observations favor the premise that the lack of immune-regulation in sarcoidosis patients will facilitate the persistence of vimentin-reactive T cells in a pro-inflammatory granuloma environment. A limitation of our study is that in sarcoidosis patients, it is challenging to determine whether anti-vimentin immune responses are the cause or consequence of an inflammatory response. Regardless, our study supports the hypothesis that an immune response to vimentin can be pathogenic in sarcoidosis.

Sarcoidosis patients show the presence of IFN γ and IL-17 producing cells in BAL, establishing a pathogenic role for TH1/TH17/TH17.1 CD4 T cell subsets [36]. A high level of IFN γ favors the formation of Langhans MGC, while IL-13/IL-4 cytokines facilitate foreign body MGC formation [37]. In addition to IFN γ and IL-17, the TH2 pathway-associated cytokine IL-33 is present in BAL from sarcoidosis patients and is detected in lung granulomas [38,39]. The function of IL-33 and other TH2 cytokines in granulomas and MGC formation in sarcoidosis is unclear. We postulate that the type 2 innate immune cells in the lungs may contribute to the TH2 pathway activation and influence early events in granuloma

formation. Lung ILC2 cells are located close to the epithelial lining of large and small airways, and these cells were significantly enriched in the BAL fluid of vimentin-immunized mice. Although the absolute numbers of ILC2 are small, they are the early responders to lung inflammation and affect the clearing of pathogens and tissue repair [40]. Analysis of BAL from sarcoidosis patients for the presence of ILC2 will substantiate their role in disease pathogenesis.

In summary, our study further validates vimentin as a legitimate autoantigen in sarcoidosis and demonstrates the pathogenic potential of anti-vimentin immune response in a pulmonary mouse model of sarcoidosis.

Author contributions

Harini Bagavant: Conceptualization, methodology, investigation, validation, formal analysis, writing – original draft, visualization. **Katarzyna Cizio:** Methodology, investigation, software. **Antonina M. Araszkievicz:** Methodology, investigation, formal analysis, writing – review and editing. **Joanna A. Papinska:** Methodology, investigation. **Lori Garman:** Investigation, validation, formal analysis, writing – review and editing. **Chuang Li:** Formal analysis, data curation. **Nathan Pezant:** Formal analysis, data curation. **Wonder P. Drake:** Resources, writing – review and editing. **Courtney G. Montgomery:** Conceptualization, resources, formal analysis, data curation, writing – review and editing. **Umesh S. Deshmukh:** Conceptualization, methodology, formal analysis, visualization, writing – original draft, funding acquisition.

Declaration of competing interest

The authors declare that they have no known competing financial interests or personal relationships that could have appeared to influence the work reported in this paper.

Acknowledgements

This study was partly funded by grants from the Foundation for Sarcoidosis Research, USA, and the Presbyterian Health Foundation, USA. The authors acknowledge the excellent technical support from the OMRF Imaging Core Facility for tissue sectioning and image acquisition, and the OMRF Flow Cytometry Core for support with data acquisition. In addition, we thank the Laboratory for Molecular Biology and Cytometry Research at Oklahoma University Health Sciences Center for using the Core Facility, which provided Nanostring gene expression service. Finally, we thank the patients who participate in sarcoidosis research and specifically those from the VUMC.

Appendix A. Supplementary data

Supplementary data to this article can be found online at <https://doi.org/10.1016/j.jtauto.2022.100153>.

References

- [1] J. Grunewald, J.C. Grutters, E.v. Arkema, L.A. Saketkoo, D.R. Moller, J. Müller-Quernheim, Sarcoidosis, *Nat. Rev. Dis. Prim.* 5 (2019) 45, <https://doi.org/10.1038/s41572-019-0096-x>.
- [2] S. Dubrey, S. Shah, T. Hardman, R. Sharma, Sarcoidosis: the links between epidemiology and aetiology, *Postgrad. Med.* 90 (2014) 582–589, <https://doi.org/10.1136/postgradmedj-2014-132584>.
- [3] J.E. Rotsinger, L.J. Celada, V.v. Polosukhin, J.B. Atkinson, W.P. Drake, Molecular analysis of sarcoidosis granulomas reveals antimicrobial targets, *Am. J. Respir. Cell Mol. Biol.* 55 (2016) 128–134, <https://doi.org/10.1165/rcmb.2015-0212OC>.
- [4] S.A. Greaves, A. Ravindran, R.G. Santos, L. Chen, M.T. Falta, Y. Wang, A. M. Mitchell, S.M. Atif, D.G. Mack, A.N. Tinega, L.A. Maier, S. Dai, C. Pinilla, J. Grunewald, A.P. Fontenot, CD4+ T cells in the lungs of acute sarcoidosis patients recognize an *Aspergillus nidulans* epitope, *J. Exp. Med.* 218 (2021) 10, <https://doi.org/10.1084/jem.20210785>.
- [5] M. Negi, T. Takemura, J. Guzman, K. Uchida, A. Furukawa, Y. Suzuki, T. Iida, I. Ishige, J. Minami, T. Yamada, H. Kawachi, U. Costabel, Y. Eishi, Localization of *Propionibacterium acnes* in granulomas supports a possible etiologic link between sarcoidosis and the bacterium, *Mod. Pathol.* 25 (2012) 1284–1297, <https://doi.org/10.1038/modpathol.2012.80>.
- [6] E.L. Clarke, A.P. Lauder, C.E. Hofstaedter, Y. Hwang, A.S. Fitzgerald, I. Imai, W. Biernat, B. Rękawiecki, H. Majewska, A. Dubaniewicz, L.A. Litzky, M. D. Feldman, K. Bittinger, M.D. Rossman, K.C. Patterson, F.D. Bushman, R. G. Collman, Microbial lineages in sarcoidosis. A metagenomic analysis tailored for low-microbial content samples, *Am. J. Respir. Crit. Care Med.* 197 (2018) 225–234, <https://doi.org/10.1164/rccm.201705-0891OC>.
- [7] J. Wahlström, J. Dengjel, O. Winqvist, I. Targoff, B. Persson, H. Duyar, H. G. Rammensee, A. Eklund, R. Weissert, J. Grunewald, Autoimmune T cell responses to antigenic peptides presented by bronchoalveolar lavage cell HLA-DR molecules in sarcoidosis, *Clin. Immunol.* 133 (2009) 353–363, <https://doi.org/10.1016/j.clim.2009.08.008>.
- [8] L.E. Siltzbach, The Kveim test in sarcoidosis. A study of 750 patients, *JAMA* 178 (1961) 476–482, <https://doi.org/10.1001/jama.1961.03040440028006>.
- [9] C. Eberhardt, M. Thillai, R. Parker, N. Siddiqui, L. Potiphar, R. Goldin, J.F. Timms, A.U. Wells, O.M. Kon, M. Wickremasinghe, D. Mitchell, M.E. Weeks, A. Lalvani, Proteomic analysis of Kveim reagent identifies targets of cellular immunity in sarcoidosis, *PLoS One* 12 (2017), e0170285, <https://doi.org/10.1371/journal.pone.0170285>.
- [10] A. Musaalayan, S. Lapin, V. Nazarov, O. Tkachenko, B. Gilburd, A. Mazing, L. Mikhailova, Y. Shoenfeld, Vimentin as antigenic target in autoimmunity: a comprehensive review, *Autoimmun. Rev.* 17 (2018) 926–934, <https://doi.org/10.1016/j.autrev.2018.04.004>.
- [11] A. Malkova, A. Starshinova, Y. Zinchenko, N. Gavrilova, I. Kudryavtsev, S. Lapin, A. Mazing, E. Surkova, M. Pavlova, E. Belaeva, T. Stepanenko, P. Yablonskiy, Y. Shoenfeld, New Laboratory Criteria of the Autoimmune Inflammation in Pulmonary Sarcoidosis and Tuberculosis, vol. 227, *Clinical Immunology*, Orlando, Fla, 2021, p. 108724, <https://doi.org/10.1016/j.clim.2021.108724>.
- [12] A.J. Kinloch, Y. Kaiser, D. Wolfgeher, J. Ai, A. Eklund, M.R. Clark, J. Grunewald, In situ humoral immunity to vimentin in HLA-drb1*03+ patients with pulmonary sarcoidosis, *Front. Immunol.* 9 (2018) 1, <https://doi.org/10.3389/fimmu.2018.01516>.
- [13] M. Drent, E.D. Crouser, J. Grunewald, Challenges of sarcoidosis and its management, *N. Engl. J. Med.* 385 (2021) 1018–1032, <https://doi.org/10.1056/NEJMra2101555>.
- [14] E.D. Crouser, L.A. Maier, K.C. Wilson, C.A. Bonham, A.S. Morgenthau, K. C. Patterson, E. Abston, R.C. Bernstein, R. Blankstein, E.S. Chen, D.A. Culver, W. Drake, M. Drent, A.K. Gerke, M. Ghobrial, P. Govender, N. Hamzeh, W. E. James, M.A. Judson, L. Kellermeier, S. Knight, L.L. Koth, V. Poletti, S.V. Raman, M.H. Tukey, G.E. Westney, R.P. Baughman, Diagnosis and detection of sarcoidosis, *Off. Am. Thorac. Soc. Clin. Pract. Guideline* 201 (2020) E26–E51, <https://doi.org/10.1164/RCCM.202002-0251ST>.
- [15] S.W. Chensue, K. Warmington, J. Ruth, P. Lincoln, M.C. Kuo, S.L. Kunkel, Cytokine responses during mycobacterial and schistosomal antigen-induced pulmonary granuloma formation. Production of Th1 and Th2 cytokines and relative contribution of tumor necrosis factor, *Am. J. Pathol.* 145 (1994) 1105–1113, <http://www.ncbi.nlm.nih.gov/pubmed/7977642>.
- [16] C.M. Swaisgood, K. Oswald-Richter, S.D. Moeller, J.M. Klemenc, L.M. Ruple, C. F. Farver, J.M. Drake, D.A. Culver, W.P. Drake, Development of a sarcoidosis murine lung granuloma model using *Mycobacterium superoxide dismutase A* peptide, *Am. J. Respir. Cell Mol. Biol.* 44 (2011) 166–174, <https://doi.org/10.1165/rcmb.2009-0350OC>.
- [17] P. Bankhead, M.B. Loughrey, J.A. Fernández, Y. Dombrowski, D.G. McArt, P. D. Dunne, S. McQuaid, R.T. Gray, L.J. Murray, H.G. Coleman, J.A. James, M. Salto-Tellez, P.W. Hamilton, QuPath: open source software for digital pathology image analysis, *Sci. Rep.* 7 (2017) 16878, <https://doi.org/10.1038/s41598-017-17204-5>.
- [18] T.C.M. Th van Maarsseveen, W. Vos, P.J. van Diest, Giant cell formation in sarcoidosis: cell fusion or proliferation with non-division? *Clin. Exp. Immunol.* 155 (2009) 476–486, <https://doi.org/10.1111/j.1365-2249.2008.03841.x>.
- [19] S.A. Greaves, S.M. Atif, A.P. Fontenot, Adaptive immunity in pulmonary sarcoidosis and chronic beryllium disease, *Front. Immunol.* 11 (2020) 474, <https://doi.org/10.3389/fimmu.2020.00474>.
- [20] A.J. Pagán, L. Ramakrishnan, the formation and function of granulomas, *Annu. Rev. Immunol.* 36 (2018) 639–665, <https://doi.org/10.1146/annurev-immunol-032712-100022>.
- [21] M. Shamaei, E. Mortaz, M. Pourabdollah, J. Garssen, P. Tabarsi, A. Velayati, I. M. Adcock, Evidence for M2 macrophages in granulomas from pulmonary sarcoidosis: a new aspect of macrophage heterogeneity, *Hum. Immunol.* 79 (2018) 63–69, <https://doi.org/10.1016/j.humimm.2017.10.009>.
- [22] L.J. Celada, J.A. Kropski, J.D. Herazo-Maya, W. Luo, A. Creecy, A.T. Abad, O. S. Chioma, G. Lee, N.E. Hassell, G.I. Shaginurova, Y. Wang, J.E. Johnson, A. Kerrigan, W.R. Mason, R.P. Baughman, G.D. Ayers, G.R. Bernard, D.A. Culver, C. G. Montgomery, T.M. Maher, P.L. Molyneaux, I. Noth, S.E. Mutsaers, C.M. Prele, R. S. Peebles, D.C. Newcomb, N. Kaminski, T.S. Blackwell, L. van Kaer, W.P. Drake, PD-1 up-regulation on CD4+ T cells promotes pulmonary fibrosis through STAT3-mediated IL-17A and TGF-β1 production, *Sci. Transl. Med.* 10 (2018) 460, <https://doi.org/10.1126/scitranslmed.aar8356>.
- [23] C. Taflin, M. Miyara, D. Nochy, D. Valeyre, J.M. Naccache, F. Altare, P. Salek-Peyron, C. Badoual, P. Bruneval, J. Haroche, A. Mathian, Z. Amoura, G. Hill, G. Gorochov, FoxP3+ regulatory T cells suppress early stages of granuloma formation but have little impact on sarcoidosis lesions, *Am. J. Pathol.* 174 (2009) 497, <https://doi.org/10.2353/AJPATH.2009.080580>.
- [24] M.A. Sallin, K.D. Kauffman, C. Riou, E. du Bruyn, T.W. Foreman, S. Sakai, S. G. Hoft, T.G. Myers, P.J. Gardina, A. Sher, R. Moore, T. Wilder-Kofie, I.N. Moore, A. Sette, C.S. Lindestam Arlehamn, R.J. Wilkinson, D.L. Barber, Host resistance to

- pulmonary Mycobacterium tuberculosis infection requires CD153 expression, *Nat. Microbiol.* 3 (2018) 1198–1205, <https://doi.org/10.1038/s41564-018-0231-6>, 11. 132018.
- [25] D.T. Gracias, G.S. Sethi, A.K. Mehta, H. Miki, R.K. Gupta, H. Yagita, M. Croft, Combination blockade of OX40L and CD30L inhibits allergen-driven memory T H 2 cell reactivity and lung inflammation, *J. Allergy Clin. Immunol.* 147 (2021) 2316–2329, <https://doi.org/10.1016/J.JACI.2020.10.037>.
- [26] V. Panova, M. Gogoi, N. Rodriguez-Rodriguez, M. Sivasubramaniam, H.E. Jolin, M. W.D. Heycock, J.A. Walker, B.M.J. Rana, L.F. Drynan, M. Hodkinson, R. Pannell, G. King, M. Wing, A.J. Easton, C.A. Oedekoven, D.G. Kent, P.G. Fallon, J.L. Barlow, A.N.J. McKenzie, Group-2 innate lymphoid cell-dependent regulation of tissue neutrophil migration by alternatively activated macrophage-secreted Ear11, *Mucosal Immunol.* 14 (2021) 26–37, <https://doi.org/10.1038/s41385-020-0298-2>.
- [27] J. Grunewald, A. Eklund, Löfgren's Syndrome, *Am. J. Respir. Crit. Care Med.* 179 (2009) 307–312, <https://doi.org/10.1164/rccm.200807-1082OC>.
- [28] F. Jeny, J.C. Grutters, Experimental models of sarcoidosis: where are we now? *Curr. Opin. Pulm. Med.* 26 (2020) 554–561, <https://doi.org/10.1097/MCP.0000000000000708>.
- [29] I. Huizar, A. Malur, Y.A. Midgette, C. Kukoly, P. Chen, P.C. Ke, R. Podila, A.M. Rao, C.J. Wingard, L. Dobbs, B.P. Barna, M.S. Kavuru, M.J. Thomassen, Novel murine model of chronic granulomatous lung inflammation elicited by carbon nanotubes, *Am. J. Respir. Cell Mol. Biol.* 45 (2011) 858–866, <https://doi.org/10.1165/rcmb.2010-0401OC>.
- [30] I. Huizar, A. Malur, J. Patel, M. McPeck, L. Dobbs, C. Wingard, B.P. Barna, M. J. Thomassen, The role of PPAR γ in carbon nanotube-elicited granulomatous lung inflammation, *Respir. Res.* 14 (2013) 7, <https://doi.org/10.1186/1465-9921-14-7>.
- [31] J.L. Werner, S.G. Escolero, J.T. Hewlett, T.N. Mak, B.P. Williams, Y. Eishi, G. Núñez, Induction of pulmonary granuloma formation by Propionibacterium acnes is regulated by MyD88 and Nox2, *Am. J. Respir. Cell Mol. Biol.* 56 (2017) 121–130, <https://doi.org/10.1165/rcmb.2016-0035OC>.
- [32] M. Linke, H.T.T. Pham, K. Katholnig, T. Schnöller, A. Miller, F. Demel, B. Schütz, M. Rosner, B. Kovacic, N. Sukhbaatar, B. Niederreiter, S. Blüml, P. Kuess, V. Sexl, M. Müller, M. Mikula, W. Weckwerth, A. Haschemi, M. Susani, M. Hengstschläger, M.J. Gambello, T. Weichhart, Chronic signaling via the metabolic checkpoint kinase mTORC1 induces macrophage granuloma formation and marks sarcoidosis progression, *Nat. Immunol.* 18 (2017) 293–302, <https://doi.org/10.1038/ni.3655>.
- [33] J. Song, M. Zhao, Q. Li, L. Lu, Y. Zhou, Y. Zhang, T. Chen, D. Tang, N. Zhou, C. Yin, D. Weng, H. Li, IL-17A can promote Propionibacterium acnes-induced sarcoidosis-like granulomatosis in mice, *Front. Immunol.* 10 (2019) 1923, <https://doi.org/10.3389/fimmu.2019.01923>.
- [34] N. Mor-Vaknin, A. Punturieri, K. Sitwala, D.M. Markovitz, Vimentin is secreted by activated macrophages, *Nat. Cell Biol.* 5 (2003) 59–63, <https://doi.org/10.1038/ncb898>.
- [35] I. Ramos, K. Stamatakis, C.L. Oeste, D. Pérez-Sala, Vimentin as a multifaceted player and potential therapeutic target in viral infections, *Int. J. Mol. Sci.* 21 (2020) 4675, <https://doi.org/10.3390/ijms21134675>.
- [36] R. Lepzien, M. Nie, P. Czarnewski, S. Liu, M. Yu, A. Ravindran, S. Kullberg, A. Eklund, J. Grunewald, A. Smed-Sörensen, Pulmonary and blood dendritic cells from sarcoidosis patients more potently induce IFN γ -producing Th1 cells compared with monocytes, *J. Leukoc. Biol.* (2021), <https://doi.org/10.1002/JLB.5A0321-162R>.
- [37] A.K. McNally, J.M. Anderson, Macrophage fusion and multinucleated giant cells of inflammation, in: *Advances in Experimental Medicine and Biology*, Adv Exp Med Biol, 2011, pp. 97–111, https://doi.org/10.1007/978-94-007-0763-4_7.
- [38] W. Naumnik, B. Naumnik, W. Niklińska, M. Ossolińska, E. Chyczewska, Interleukin-33 as a new marker of pulmonary sarcoidosis, *Adv. Exp. Med. Biol.* 866 (2015) 1–6, https://doi.org/10.1007/5584_2015_142.
- [39] W. Kempf, T. Zollinger, M. Sachs, E. Ullmer, G. Cathomas, S. Dirnhofer, K.D. Mertz, Granulomas are a source of interleukin-33 expression in pulmonary and extrapulmonary sarcoidosis, *Hum. Pathol.* 45 (2014) 2202–2210, <https://doi.org/10.1016/J.HUMPATH.2014.07.011>.
- [40] S. Wirtz, A. Schulz-Kuhnt, M.F. Neurath, I. Atreya, Functional contribution and targeted migration of group-2 innate lymphoid cells in inflammatory lung diseases: being at the right place at the right time, *Front. Immunol.* 12 (2021) 688879, <https://doi.org/10.3389/fimmu.2021.688879>.